Evaluation of an experimental electrohydraulic discharge device for extracorporeal shock wave lithotripsy: Pressure field of sparker array

Guangyan Li
School of Physics, Northeast Normal University, Changchun, 130024, People's Republic of China

Bret A. Connors[a)]
Department of Anatomy and Cell Biology, Indiana University School of Medicine, Medical Science Building, Room 0051, 635 Barnhill Drive, Indianapolis, Indiana 46202, USA

Ray B. Schaefer
Phoenix Science and Technology, C/O John Gallagher, 12 Van Buren Circle, Goffstown, New Hampshire 03045, USA

John J. Gallagher
Phoenix Science and Technology, 12 Van Buren Circle, Goffstown, New Hampshire 03045, USA

Andrew P. Evan
Department of Anatomy and Cell Biology, Indiana University School of Medicine, Medical Science Building, Room 0051, 635 Barnhill Drive, Indianapolis, Indiana 46202, USA

(Received 14 April 2017; revised 8 September 2017; accepted 27 October 2017; published online 20 November 2017)

In this paper, an extracorporeal shock wave source composed of small ellipsoidal sparker units is described. The sparker units were arranged in an array designed to produce a coherent shock wave of sufficient strength to fracture kidney stones. The objective of this paper was to measure the acoustical output of this array of 18 individual sparker units and compare this array to commercial lithotripters. Representative waveforms acquired with a fiber-optic probe hydrophone at the geometric focus of the sparker array indicated that the sparker array produces a shock wave (P^+ ~40–47 MPa, P^- ~2.5–5.0 MPa) similar to shock waves produced by a Dornier HM-3 or Dornier Compact S. The sparker array's pressure field map also appeared similar to the measurements from a HM-3 and Compact S. Compared to the HM-3, the electrohydraulic technology of the sparker array produced a more consistent SW pulse (shot-to-shot positive pressure value standard deviation of ±4.7 MPa vs ±3.3 MPa). © *2017 Acoustical Society of America*.
https://doi.org/10.1121/1.5010901

[KAW] Pages: 3147–3153

I. INTRODUCTION

Shock wave lithotripsy (SWL) was introduced in the early 1980s and rapidly became the method of choice for the treatment of urinary stones.[1,2] The first lithotripter employed in the United States was the Dornier HM-3, which utilized a spark gap electrode to produce a shock wave (SW) used to pulverize stones into fragments of passable size. After the debut of the HM-3, several other manufacturers introduced lithotripter models that featured spark gap electrodes, as well as machines that incorporated newer electromagnetic or piezoelectric SW generator technology. However, many considered the HM-3 to be the "gold standard" of lithotripters,[3–5] and sought to improve on the SW generating technology of that machine.

For the HM-3, the SW was generated by the rapid discharge of energy across the electrode tips of an underwater spark gap. The spherical SW produced at that gap was then reflected by a hemi-ellipsoidal bowl towards the focal zone. Unfortunately, the electrodes of the HM-3 degraded due to erosion and vaporization by the spark. The increase in spark gap separation not only reduced the power of the SW, but also increased shock-to-shock variability, and consequently altered the acoustic pressure profile at the focus. To overcome these shortcomings, work has centered on improving the spark system by adjusting the spark gap after a certain number of firings[6,7] or by encapsulating the electrode in an highly conductive electrolyte-filled housing which channeled the discharge between the two electrodes.[8,9] In this paper we present information on a new technique to generate a focused SW that involves the use of small ellipsoidal sparker units. The objective of the current study was to measure the acoustical output of an array of these sparker units (Phoenix Science and Technology sparker array, SPA) and compare this array to commercial lithotripters. This analysis will be used to help evaluate whether an array of these sparker units have the potential to produce a SW suitable for use in a clinical lithotripter.

[a)]Electronic mail: bconnors@iupui.edu

II. MATERIALS AND METHODS

A. Ellipsoidal sparker unit

Each individual sparker unit (Fig. 1 and Fig. 2 inset) consists of a central electrode (1.27 mm diameter) made of stainless steel with a flat surface facing the focal point. Surrounding the electrode is an insulator piece (6.73 mm diameter) made of Delrin AF (volume resistivity of $3.0 \times 10^{16}\,\Omega\,\text{cm}$). This assembly is surrounded by a small brass hemi-ellipsoid of 20.2 mm in diameter and comprises ≈11% of the hemi-ellipsoid (89% of the hemi-ellipsoid has been removed). The focal distance of each sparker unit is 181.6 mm. In order for the sparker units to work the sparkers are immersed in salt water with a conductivity of ∼5 S/m, which is similar to seawater. At the time of an electrical discharge, electrical breakdown occurs between the face of the electrode and this solution. The resulting vapor bubble produces the SW from each sparker. Unlike other electrohydraulic shock sources used for extracorporeal SWL, the sparker units do not have a spark gap. This is a unique feature of this SW generating system. A second electrode is located behind the sparker array sphere and is immersed in the same solution as the sparker unit electrode, thus completing the circuit. Because the solution is so conductive and because the brass reflector is insulated and does not create a current path between the 2 electrodes, the electrical discharge only occurs at the face of the central electrode.

B. Sparker array design

Currently, the majority of extracorporeal SW lithotripters on the market consist of machines with a dry-head design. Integral to this design is a treatment head bellows that is placed against the patient during treatment. A bellows (Dornier MedTech America, Kennesaw, GA) was obtained of approximately 267 mm in diameter. The size of the bellows dictated the design size of the SPA treatment head. The individual sparker units were arranged on the concave surface of a thick plastic partial sphere so that each sparker was at the same distance from the focal point. This focal length from the surface of the partial sphere to the SW focus was 181.6 mm. In the space available in a 267 mm diameter concave surface it was determined that a maximum number of 27 sparker units would fit into this area. The 27 sparker units were further divided into three groups of nine sparkers (Fig. 2). Each group of nine sparker units was clustered together so that each group covered 1/3 of the array surface forming a wedge shape with the apex at the center of the array and the base at the outer rim of the array. The boundaries between the wedges were at 2, 6, and 10 o'clock.

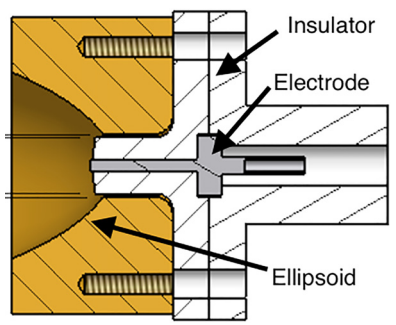

FIG. 1. (Color online) Diagram of individual sparker unit in cross-section. The electrode appears elongated and is in the center of the diagram (dark). The electrode protrudes into the brass hemi-ellipsoid (gray), with the ellipsoid opening on the left. The remaining white striped area represents the insulator.

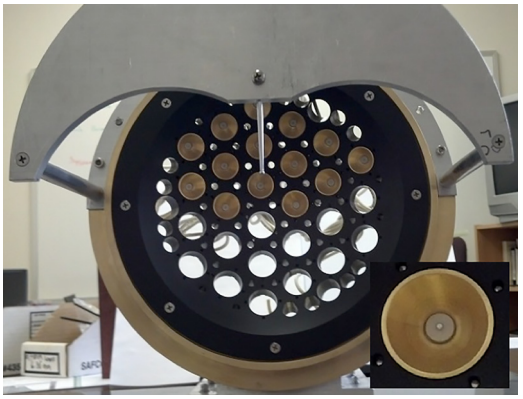

FIG. 2. (Color online) Photograph of the SPA partially assembled. Fourteen of the 27 sparkers units are installed, with openings for the remaining 13 sparker units. The smaller holes allow for water flow during operation. The half-moon shaped metal piece with the pointer is for positioning the array, where the tip of the pointer is at the mutual focus of all the sparker units. A magnified view of one of the individual sparker units is shown as an inset.

The concept of sparker groups mentioned above is important because for all tests of the SPA only the lower two groups of sparker units were fired. Each group of nine sparker units has the potential to be triggered independently of the other groups. In the original concept of the SPA, it was anticipated that the SPA may be used to produce dual-pulse SWs during each treatment pulse. However, at the time of the pressure field measurements of the SPA SWs, problems with triggering of dual-pulses prevented testing of the machine in dual-pulse mode. It was decided that only two groups of sparker units (fired simultaneously) should be evaluated to provide baseline pressure field measurements during the initial testing and evaluation of the SPA.

The high voltage system of the SPA consisted of a Kaiser Systems DC power supply (30 kV, 1500 W, Beverly, MA) which supplied ≈ 27 000 V DC to the capacitors, and three fixed General Atomics capacitors (model 31158, 1 μF rating at 40 kV, San Diego, CA). Each capacitor was intended to provide enough energy for one group of sparker units. Capacitance was set at 0.49 μF for all tests. The high voltage switch was comprised of an EG&G Electro Optics SD32-B switch (gap type, Salem, MA) triggered by an EG&G Electro Optics TM-11 A (Salem, MA) trigger module. All individual sparker units were wired in parallel from the high voltage switch. Also, to assure that all capacitors were fully charged prior to SW discharge, a firing rate of 1 Hz was used for all tests.

The SPA treatment head was designed to be mounted onto the frame of a Dornier Compact S electromagnetic lithotripter (Dornier MedTech, Kennesaw, GA). The normal Compact S treatment head was removed from its mounting plate and the SPA head was mounted in its place (Fig. 3). The SPA head did not use the water or electrical charging

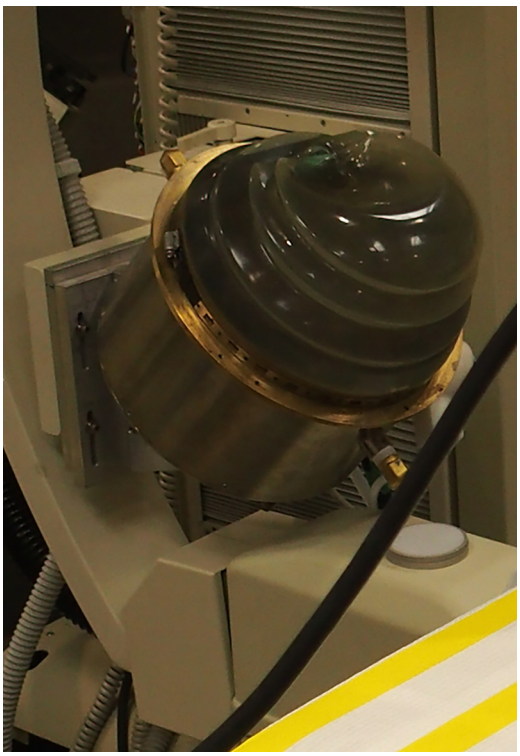

FIG. 3. (Color online) Photograph of SPA treatment head mounted on the frame of a Dornier Compact S. The x-ray source is located just below the SPA head.

system of the Compact S, but used its own dedicated systems to control for both of those functions. Mounting the SPA treatment head to the Compact S allowed the built in x-ray C-arm of the Compact S to be used to locate the geometric focus of the SPA head. The x-ray axis of the C-arm was aligned with the focal point of the SPA.

C. Acoustic measurements

The experimental setup for the acoustic measurements is illustrated in Fig. 4. The lithotripter head was coupled to the acoustic window (0.13-mm-thick Mylar film, 20 cm × 20 cm) of an acrylic tank (length 50 cm × width 52 cm × depth 40 cm) with LithoClear® coupling gel (Next Medical Products, Branchburg, NJ). The tank contained deionized water (21 °C – 23 °C) degassed to 25%–35% oxygen saturation using a multi-pinhole degasser.[10,11] The combination of thin Mylar film and the LithoClear® gel was nearly acoustically transparent to SWs.[12] Acoustic pressures were measured using a fiber-optic probe hydrophone (FOPH-500, RP Acoustics, Leutenbach, Germany) mounted on an X-Y-Z micro positioner.

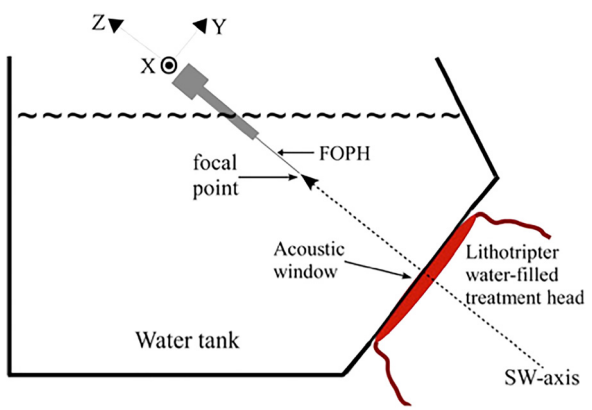

FIG. 4. (Color online) Acoustic measurements were conducted in a water-filled test tank using a fiber-optic probe hydrophone (FOPH-500) mounted on an X-Y-Z positioner. The treatment head of the SPA was coupled to the acoustic window (thin Mylar film) using LithoClear® ultrasound gel.

The SPA was set to a power level of 21.6 kV, and fired at a rate of 1 Hz. Sets of 10 or 25 waveforms (8 ns sampling rate, 5000 data points per SW) were stored using a Tektronix digital oscilloscope (TDS 5034, Tektronix, Beaverton, OR) for post processing.[13] For mapping of the acoustic field the FOPH tip was moved in steps of 1 or 2 mm along the X-axis (horizontal), Y-axis, or Z-axis (acoustic axis) over a total excursion of about 10–20 mm around the lithotripter focus. Waveforms distorted by strong cavitation were easily identified and rejected by visual inspection. The average waveforms were calculated by aligning pulses to the coincidence of the middle of the fast rising shock part of the shock wave tracing. This is a modification of the technique of aligning at the half amplitude point of the overall shock front amplitude.[10] Unless otherwise stated, pressure values were averaged over 10 waveforms at each stop during mapping. Vertical error bars indicate one standard deviation for the values of those 10 waveforms.

III. RESULTS

As stated earlier, the acoustic data were acquired with the SPA head firing two out of the three banks of sparkers at a power level of 21.6 kV. Acoustic field characterization data have also been included for the Dornier HM-3 (electrohydraulic) and Dornier Compact S (electromagnetic) lithotripters for comparison purposes using the same experimental setup. Acoustic waveforms of the sparker array head are presented first followed by acoustic mapping data for the three lithotripters.

A. Representative pressure waveforms for the sparker array

Representative waveforms acquired with the FOPH fiber tip at the focus, 5.0 mm off-focus and 10.0 mm off-focus are shown in Fig. 5. Panel 5(a) represents a pressure tracing averaged over 10 waveforms. Panel 5(b) shows five consecutive individual waveforms illustrating the shot-to-shot variability of the SPA. The focal waveform [black trace, Figs. 5(a) and 5(c)] shows that the pressure gradually increases for about 2–3 μs where the pressure reaches approximately 17.5 MPa. After that point, there is a strong fast-rising shock which reaches a peak positive pressure (P^+) of ~41.5 MPa in these waveforms. Ignoring the details of the waveforms, the overall duration of the compressional (positive pressure) phase and that of the trailing tensile (negative pressure) phase were similar and both were ~5 μs long.

Off-focus waveforms are depicted in Fig. 5(c) along with a standard at-focus pressure tracing. The off-focus pressure waveforms show similar temporal characteristics to the

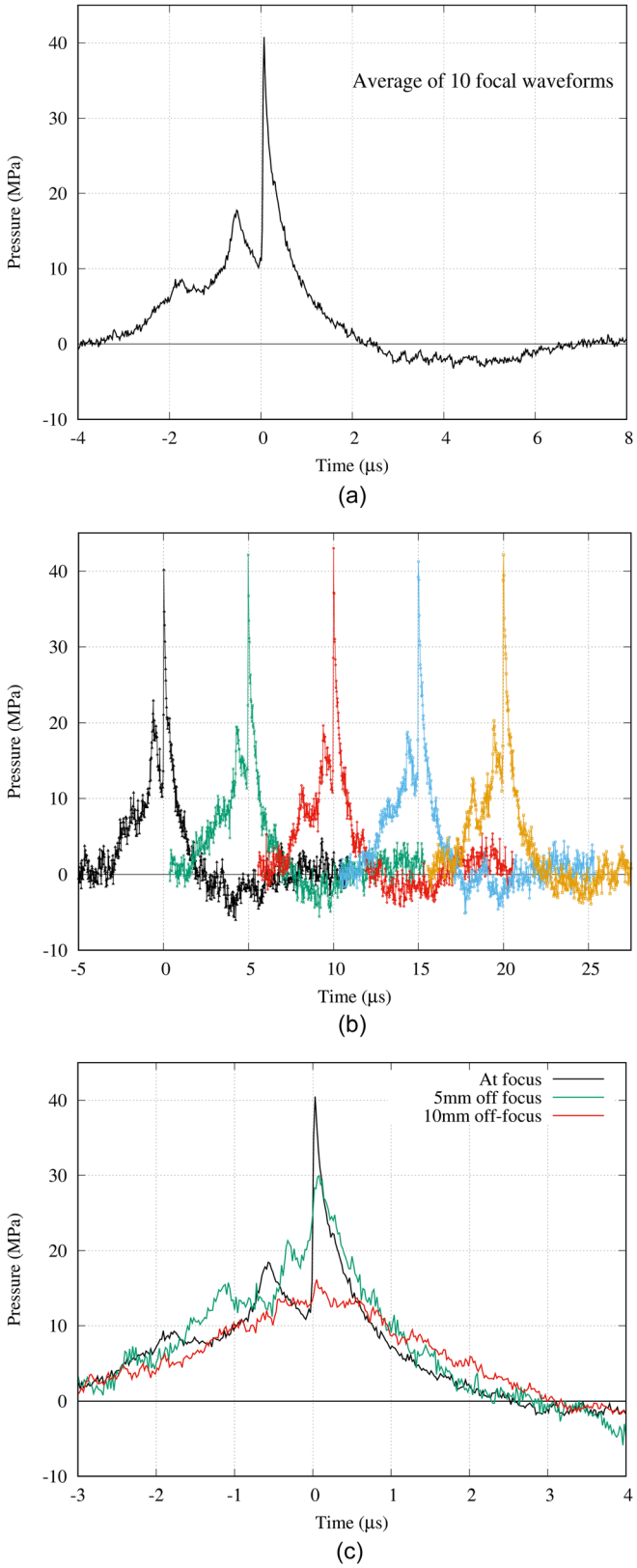

FIG. 5. (Color online) Representative pressure waveform (averaged over 10 shots) when the FOPH fiber tip was placed at the geometric focus [Panel (a)]. Panel (b) shows 5 consecutive individual pressure waveforms arranged on single graph. Note that each individual waveform shows a similar gradual pressure increase preceding the fast-rising shock front. Panel (c) includes waveforms measured at the focus (dark line), 5 mm (light gray) and 10 mm (darker gray) off-axis along the Y-axis. In those waveforms there is a fall in peak pressure as you move away from the geometric focus.

waveform at-focus, but have a much weaker shock (P^+ of ~30 MPa), as noted in the example of the pressure trace at 5 mm off-axis (lighter gray line). This weaker shock is due to the off-focus point being away from the focus of all of the sparker units. As expected, the pressure peak of the 10 mm off-axis trace (darker gray line) is lower than the 5 mm off-axis position, and there is little indication of a steep shock front.

Comparison of the focal waveforms for the Phoenix SPA, the Dornier HM-3 and Compact S lithotripters are demonstrated in Fig. 6. The HM-3 was fired at 18 kV and the Compact-S was set to a medium power level of 3 (~13 kV). Both the HM-3 and Compact S can typically reach pressure values of about 55 MPa, while the SPA operating at 21.6 kV reached 40 MPa in this example. All three lithotripters show similar focal waveforms except that the SPA has a prolonged rise time prior to the rapid rise of the main shock front. The representative waveform of the HM-3 also shows a secondary pressure peak, but this peak follows the main peak and is thought to be caused by the cutouts in the ellipsoid for the x-ray system. The tensile portion of waveforms for the different lithotripters look alike and all are about ~3–5 μs long.

B. Acoustic mapping results

Mapping of the pressure field along the horizontal X-axis in the focal plane is shown in Fig. 7. Both the P^+ and P^- mappings were acquired using the same set of pressure data. Negative pressure values here and in the Y- and Z-axis show larger relative variability than the corresponding positive pressure values. Even with a FOPH hydrophone, that has better negative pressure rendition than polyvinylidene fluoride (PVDF) based hydrophones, measurement of the negative pressures of lithotripter SWs is always difficult. This difficulty arises because water conditions such as gas content and purity can have a significant effect on measurements.[14]

The acoustic profile of the SPA is supposed to be axisymmetric when its geometrically symmetrical sparkers are

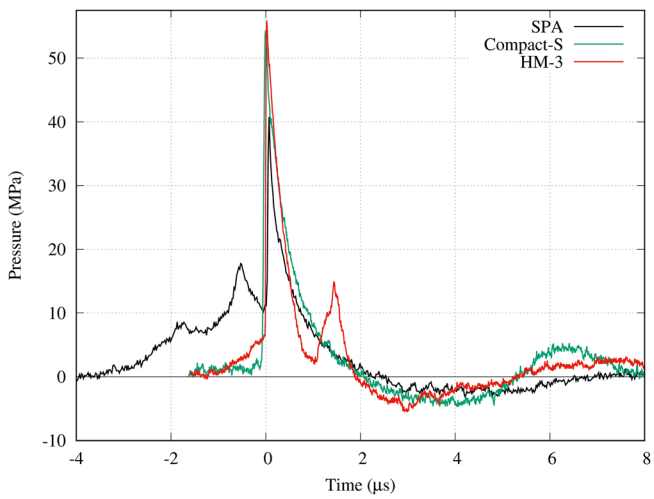

FIG. 6. (Color online) Comparison of focal waveforms for the Phoenix SPA, the Dornier HM-3 and Dornier Compact S. All pressure waveforms were acquired using the same experimental setup and were averaged over ~10 SWs. Note that waveforms were purposely aligned at the shock front for comparison purposes.

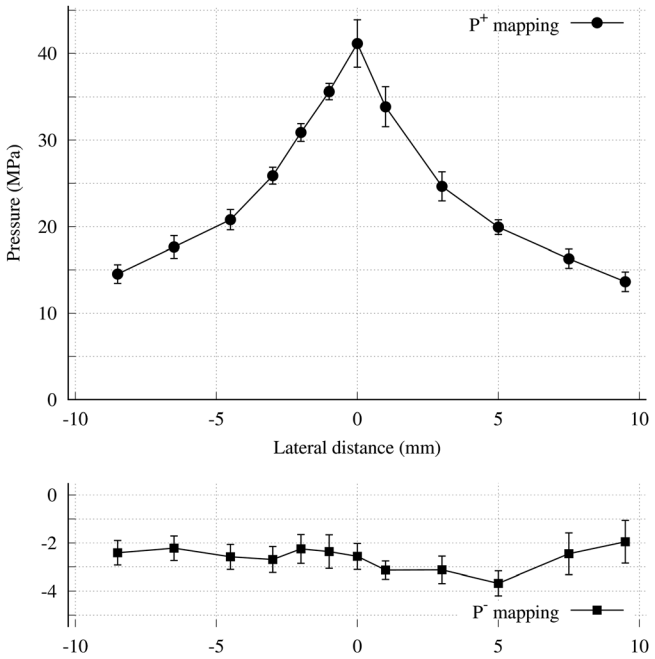

FIG. 7. The peak positive pressure (P^+) and peak negative pressure (P^-) mapping data along the X-axis in the focal plane. The 0 coordinate represents the point of the geometric focus. Vertical error bars indicate one standard deviation for values computed over ∼10 waveforms that were collected at each location during mapping.

all firing at the same time. But, when only two out of three banks of sparkers are fired the field becomes asymmetric along the Y-axis. This asymmetry is most evident in the P^+ data in Fig. 8.

Mapping along the acoustic axis (Z-axis) of the SPA head was also performed (Fig. 9). The SPA appears to

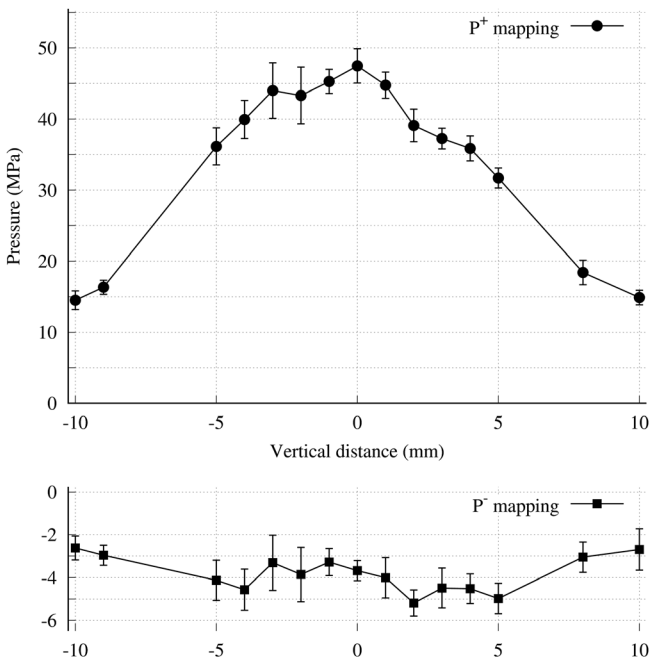

FIG. 8. The P^+ and P^- mapping data along the vertical Y-axis in the focal plane. The 0 coordinate represents the point of the geometric focus. Vertical bars indicate one standard deviation for values computed over ∼10 waveforms that were collected at each location during mapping.

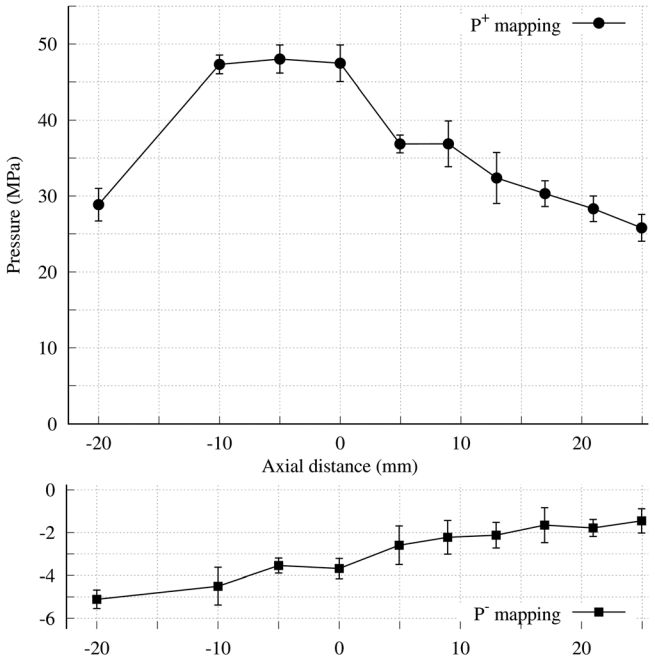

FIG. 9. The P^+ and P^- mapping data along the Z-axis (acoustic axis). The 0 coordinate represents the point of the geometric focus. Vertical bars indicate one standard deviation for computed values over ∼10 waveforms that were collected at each location during mapping.

produce a large P^+ and P^- pressure in front of the geometric focus. Interestingly, other researchers have observed that P^- peaks in front of the geometric focus[15–17] or that peak P^- precedes the peak in P^+ along the Z-axis in some electrohydraulic lithotripters.[18]

C. Lithotripter comparisons

Comparison of the acoustic fields for the three lithotripters was conducted by overlaying the acoustic mapping data along the Y-axis (Fig. 10). For the SPA, measurements along its −Y axis are the most accurate representation of the pressure field, since both of the lower groups of sparkers are firing. If you go in the +Y direction or if you measure along the −X or +X direction the pressure field is reduced due to the top group of sparkers not being fired. The HM-3 and Compact S do not exhibit this asymmetry in their pressure field due to the design of those machines. In order to estimate the width of the focal zone of the SPA the pressure measurements along the −Y axis were duplicated along the +Y axis to create a mirror image of the pressure field with respect to the geometric focus. This manipulation was done solely to gain a more complete idea of the acoustic field of the SPA for comparison purposes in Fig. 10, and should not be confused with the mapping of the Y pressure field in Fig. 8. The discharge voltages used for the HM-3 and Compact S were chosen so that the P^+ pressure at the geometric focus were similar to the SPA. Using the modification of the pressure field mentioned above, the estimated half maximum focal width of the SPA is in the range of 13–15 mm which appears wider than both the HM-3 and the Compact S. The P^- mappings of all three machines shows that the P^- pressure fields have similar P^- values (range from −3.3 to

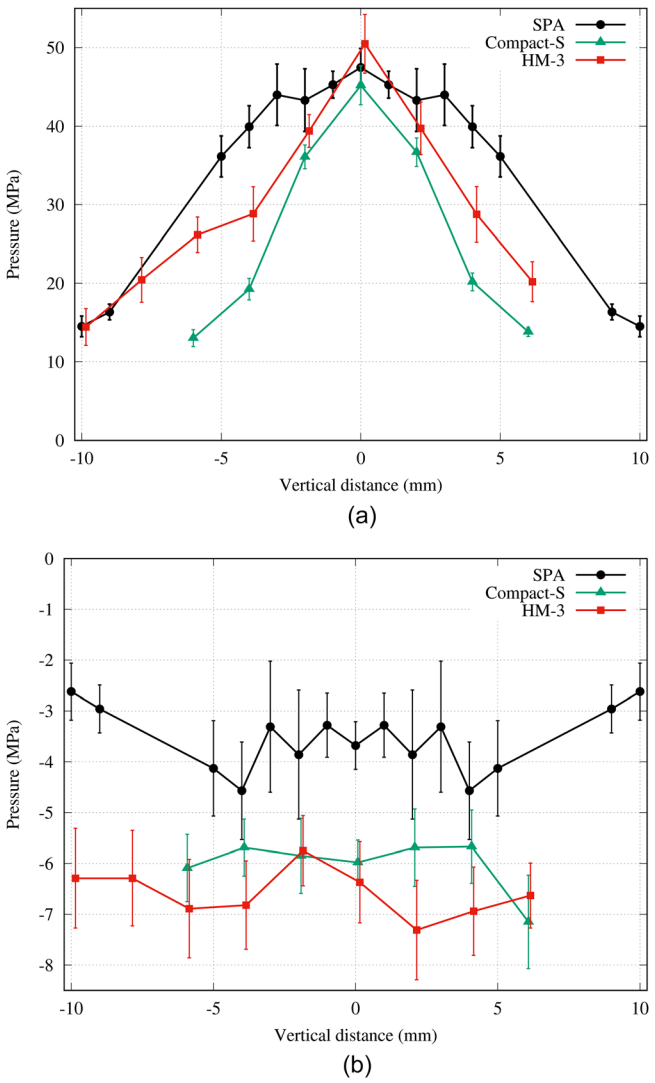

FIG. 10. (Color online) Comparison of the P^+ [Panel (a)] and the corresponding P^- [Panel (b)] mapping of the Phoenix SPA, the Dornier HM-3 and Dornier Compact S along the Y-axis. The 0 coordinate represents the point of the geometric focus. In order to estimate the width of the focal zone of the SPA the pressure measurements along the −Y axis were duplicated along the +Y axis to create a mirror image of the pressure field with respect to the geometric focus. This manipulation was done solely to gain a more complete idea of the acoustic field of the SPA for comparison purposes. Vertical bars indicate one standard deviation for values computed over ∼10 waveforms that were collected at each location during mapping.

−7.3 MPa within 5 mm of the geometric focus) and similar amounts of shot-to-shot variability (±0.5 to ±1.3 MPa for the SPA, ±0.7 to ±1.4 MPa for the HM-3, and ±0.5 to ±0.8 MPa for the Compact S).

IV. DISCUSSION

The underwater spark gap technology used by the Dornier HM-3 fractured renal stones well.[3–5] However, due to electrode erosion at the spark gap as the sparkplugs are fired, the power of the HM-3's SWs declined and the shock-to-shock variability of the acoustic pressure profile increased. To improve on these shortcomings we designed a lithotripter using an array of sparker units that delivers more consistent SWs than the HM-3. Additionally, the SPA appears to have a focal width at least as wide as the HM-3.

The SPA's focal pressure waveform shows that the pressure increases gradually for about 2–3 μs prior to a large fast-rising shock front [Fig. 5(a)]. This gradual pressure increase before the steep shock front is most likely due to variability in the firing of a few individual sparker units (i.e., jitter), on the order of 1 μs or so, resulting in the early arrival of shock waves from those individual units. Another potential source contributing to the recorded gradual rise in pressure is pressure from the direct wave produced by the individual sparker units. The direct wave in the SPA usually precedes the main shock by 2–2.5 μs and measures about 14% as large as the steep shock front peak pressure.

Starting from the large shock front, the focal waveform of the SPA looks similar to those of the HM-3 and the Compact S (Fig. 6). The highest average pressure observed at the geometric focus for the SPA was 47.0 ± 3.3 MPa. In terms of pressure tracings, the SPA was slightly lower than the other two lithotripters whose positive pressure values both reached 55 MPa. Shot-to-shot positive pressure variability was measured using standard deviation values at the focus of each lithotripter. The electromagnetic Compact S had the lowest variability ±2.5 MPa, while the electrohydraulic HM-3 had the highest variability of ±4.7 MPa. The SPA, with a shot-to-shot pressure variability of ±3.3 MPa, delivered more consistent SWs than the HM-3. This result is likely due to the fact that variations in individual pressure waves produced by each of the sparker units are being averaged out by summation of the pressure waves over all 18 sparker units. The measured negative pressure values for the SPA varied from −2.5 to −5.0 MPa. These values were similar to the HM-3 and Compact S which produced negative pressures of around −6.0 to −7.0 MPa.

The pressures at the focus do not tell the whole story about a lithotripter. The focal width of the SPA appears wider than similar measurements for the Compact S and HM-3 (Fig. 10).[12] This broad focal width may be of some value since lithotripters with wide focal widths are reported to break stones effectively.[2,19] This reported improvement in stone breakage may be due to the theoretical consideration that broad focal width SWs enhance shear stress contributing to increased stone breakage[20,21] or to the practical consideration that a broad focal width allows a stone to remain in the SW focal zone even if it is moving due to respiratory excursions.[22,23]

Although not readily apparent the design of the SPA treatment head holds the potential to be quite versatile. This is in reference to several recent technological trends in lithotripter design which hold great promise for improving the outcomes of SWL treatment in the clinic.[24] One such trend, the dual-head/dual-source lithotripter which produces a dual-pulse SW, has been shown to break stones effectively by modifying the waveform of the SW and manipulating the cavitation field near the stone when compared to conventional single pulse techniques.[25] Because the SPA is made up of individual sparker units which can be fired as a group, future developments may allow the groups to be independently triggered to form dual-pulse SWs, or all sparker groups can be fired simultaneously to deliver maximum pressures to the focal region. A second trend, the use of

ultrasound probes to monitor and improve stone targeting, as well as monitor stone comminution, has the potential to reduce the number of SWs needed during treatment. For the SPA, the flexible placement of individual sparkers allows space for an in-line ultrasound probe to be mounted inside of the treatment head to achieve this same stone monitoring.

V. CONCLUSIONS

Overall, the Phoenix SPA generates very consistent waveforms with peak pressures in the range of ∼40–47 MPa (positive) and ∼−2.5–5.0 MPa (negative). Mapping of the acoustic field shows that its focal width of 13–15 mm appears to be larger than the Dornier HM-3 or Compact S, categorizing it as a mid to wide focal width lithotripter. The SPA's pressure tracings and pressure field map appear very similar to the measurements from two different commercial lithotripters (Dornier HM-3 and Compact S). Compared to the HM-3, the electrohydraulic technology of the SPA produces more consistent SW pulses (shot-to-shot positive pressure value standard deviation of ±4.7 vs ±3.3 MPa). The SPA appears to be a viable lithotripter warranting further study.

ACKNOWLEDGMENTS AND DISCLOSURE

This work was supported by National Institutes of Health Grants Nos. PO1 DK-43881 and R44 DK-089703. R.B.S. and J.J.G. have a financial interest in the Phoenix sparker array lithotripter.

[1]C. Chaussy, E. Schmiedt, D. Jocham, W. Brendel, B. Forssmann, and V. Walther, "First clinical experience with extracorporeally induced destruction of kidney stones by shock waves," J. Urol. **127**, 417–420 (1982).
[2]J. J. Rassweiler, T. Knoll, K.-U. Köhrmann, J. A. McAteer, J. E. Lingeman, R. O. Cleveland, M. R. Bailey, and C. Chaussy, "Shock wave technology and application: An update," Eur. Urol. **59**, 784–796 (2011).
[3]J. J. Rassweiler, G. G. Tailly, and C. Chaussy, "Progress in lithotripter technology," EAU Update Ser. **3**, 17–39 (2005).
[4]V. A. Leitao, W. N. Simmons, Y. Zhou, J. Qin, F. H. Cocks, J. Fehre, B. Granz, R. Nanke, G. M. Preminger, and P. Zhong, "*In vitro* comparison between HM-3 and Modularis lithotripters," AIP Conf. Proc. **900**, 372–376 (2006).
[5]J. E. Lingeman, "Lithotripsy systems," in *Smith's Textbook of Endourology*, 2nd ed., edited by A. D. Smith, G. Badlani, D. Bagley, R. V. Clayman, S. G. Docimo, G. H. Jordan, L. R. Kavoussi, B. R. Lee, J. E. Lingeman, G. M. Preminger, and J. W. Segura (BC Decker Inc, Hamilton, 2007), Chap. 39, pp. 333–342.
[6]I. Manousakas, S.-M. Liang, L.-R. Wan, and C.-H. Wang, "Development of a system of automatic gap-adjusted electrodes for shock wave generators," Rev. Sci. Instrum. **75**(11), 4811–4819 (2004).
[7]Y. A. Pishchalnikov, J. A. McAteer, J. C. Williams, B. A. Connors, R. K. Handa, J. A. Lingeman, and A. P. Evan, "Evaluation of the LitoGold LG-380 lithotripter: *In vitro* acoustic characterization and assessment of renal injury in the pig model," J. Endourol. **27**(5), 631–639 (2013).
[8]D. Cathignol, J. Mestas, F. Gomez, and P. Lenz, "Influence of water conductivity on the efficiency and the reproducibility of electrohydraulic shock wave generation," Ultrasound Med. Biol. **17**, 819–828 (1991).
[9]M. Bourlion, P. Dancer, F. Lacoste, J. L. Mestas, and D. Cathignol, "Design and characterization of a shock wave generator using canalized electrical discharge: Application to lithotripsy," Rev. Sci. Instrum. **65**(7), 2356–2363 (1994).
[10]Y. A. Pishchalnikov, J. S. Neucks, R. J. VonDerHaar, I. V. Pishchalnikova, J. C. Williams, and J. A. McAteer, "Air pockets trapped during routine coupling in dry head lithotripsy can significantly decrease the delivery of shock wave energy," J. Urol. **176**, 2706–2710 (2006).
[11]J. S. Neucks, Y. A. Pishchalnikov, A. J. Zancanaro, J. N. VonDerHaar, J. C. Williams, and J. A. McAteer, "Improved acoustic coupling for shock wave lithotripsy," Urol. Res. **36**, 61–66 (2008).
[12]G. Li, J. C. Williams, Y. A. Pishchalnikov, Z. Liu, and J. A. McAteer, "Size and location of defects at the coupling interface affect lithotripter performance," BJU Int. **110**, E871–877 (2012).
[13]Y. A. Pishchalnikov, J. A. McAteer, R. J. VonDerHaar, I. V. Pishchalnikova, J. C. Williams, and A. P. Evan, "Detection of significant variation in acoustic output of an electromagnetic lithotriptor," J. Urol. **176**, 2294–2298 (2006).
[14]Y. A. Pishchalnikov, J. A. McAteer, and J. C. Williams, "Effect of firing rate on the performance of shock wave lithotriptors," BJU Int. **102**, 1681–1686 (2008).
[15]M. A. Averkiou and R. O. Cleveland, "Modeling of an electrohydraulic lithotripter with the KZK equation," J. Acoust. Soc. Am. **106**, 102–112 (1999).
[16]R. O. Cleveland, M. R. Bailey, N. Fineberg, B. Hartenbaum, M. Lokhandwalla, J. A. McAteer, and B. Sturtevant, "Design and characterization of a research electrohydraulic lithotripter patterned after the Dornier HM3," Rev. Sci. Instrum. **71**, 2514–2525 (2000).
[17]D. L. Sokolov, M. R. Bailey, L. A. Crum, P. M. Blomgren, B. A. Connors, and A. P. Evan, "Prefocal alignment improves stone comminution in shockwave lithotripsy," J. Endourol. **16**, 709–715 (2002).
[18]M. R. Bailey, D. T. Blackstock, R. O. Cleveland, and L. A. Crum, "Comparison of electrohydraulic lithotripters with regid and pressure-release ellipsoidal reflectors. I. Acoustic fields," J. Acoust. Soc. Am. **104**, 2517–2523 (1998).
[19]W. Eisenmenger, X. Du, C. Tang, S. Zhao, Y. Wang, F. Rong, D. Dai, M. Guan, and A. Qi, "The first clinical results of wide-focus and low-pressure ESWL," Ultrasound Med. Biol. **28**, 769–774 (2002).
[20]W. Eisenmenger, "The mechanisms of stone fragmentation in ESWL," Ultrasound Med. Biol. **27**, 683–693 (2001).
[21]O. A. Sapozhnikov, A. D. Maxwell, B. MacConaghy, and M. R. Bailey, "A mechanistic analysis of stone fracture in lithotripsy," J. Acoust. Soc. Am. **121**, 1190–1202 (2007).
[22]R. O. Cleveland, R. Anglade, and R. K. Babayan, "Effect of stone motion on *in vitro* comminution efficiency of Storz Modulith SLX," J. Endourol. **18**, 629–633 (2004).
[23]M. D. Sorensen, M. R. Bailey, A. R. Shah, R. S. Hsi, M. Paun, and J. D. Harper, "Quantitative assessment of shockwave lithotripsy accuracy and the effect of respiratory motion," J. Endourol. **26**, 1070–1074 (2012).
[24]J. E. Lingeman, J. A. McAteer, E. Gnessin, and A. P. Evan, "Shock wave lithotripsy: Advances in technology and technique," Nat. Rev. Urol. **6**, 660–670 (2009).
[25]D. L. Sokolov, M. R. Bailey, and L. A. Crum, "Dual-pulse lithotripter accelerates stone fragmentation and reduces cell lysis *in vitro*," Ultrasound Med. Biol. **29**, 1045–1052 (2003).